

# A 800 Mbps and 12.37 ps Jitter Bidirectional Mixed-Voltage I/O Buffer With Dual-Path Gate-Tracking Circuit

Chua-Chin Wang, *Senior Member, IEEE*, Chih-Lin Chen, *Student Member, IEEE*, Hsin-Yuan Tseng, Hsiao-Han Hou, and Chun-Ying Juan

**Abstract**—This paper proposes a high speed bidirectional mixed-voltage I/O buffer using 90 nm 1.2 V standard CMOS process. By using a dynamic gate bias generator to provide appropriate gate drive voltages for the output stage, the I/O buffer can transmit/receive  $2 \times V_{DD}$  voltage level signal without any gate-oxide overstress hazard. Most important of all, the gate-oxide overstress hazard is eliminated by adopting a dual-path gate-tracking circuit. The maximum data rate and jitter are measured to be 800 Mbps/12.37 ps and 704 Mbps/14.79 ps for 1.2 V and 2.5 V signal voltage, respectively, with a given capacitive load of 20 pF.

**Index Terms**—Dual-path gate-tracking circuit, floating N-well circuit, gate-oxide reliability, I/O buffer, mixed-voltage-tolerant.

## I. INTRODUCTION

WITH the rapid development of semiconductor technologies, the dimensions and supply voltages of the integrated circuit (IC) are evolved to nano-meter scale so as to reduce the area cost and power consumption [1]. During such an evolution, many chips in a PCB-based system are fabricated by different technologies to meet the requirements of various interfacing specifications, e.g., PCI-X and PCI-express. A signal voltage level compatibility problem appears when those chips are used to communicate with one another, since the voltage levels of these chips might be different. Traditional I/O buffers are no longer adequate to these different voltage-level signals due to the hazards of gate-oxide overstress, hot-carrier degradation, and unwanted leakage current paths [1]–[5]. By contrast, mixed-voltage I/O buffers are considered as a better solution to

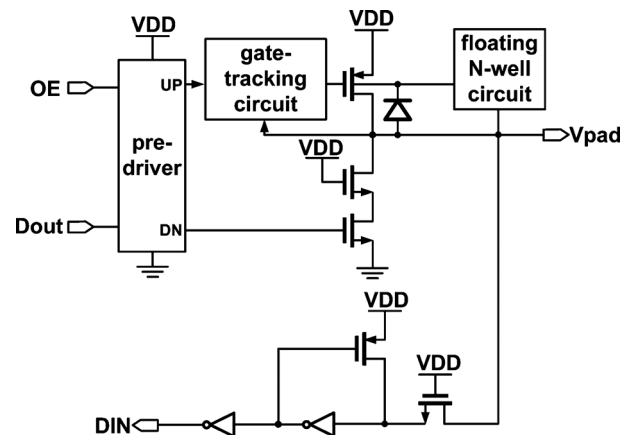


Fig. 1. Type I mixed-voltage I/O buffer with the gate-tracking and floating N-well circuits.

reduce the time-to-market than extra off-chip level shifters. Another advantage is the reduction of PCB area thanks to the removal of the voltage level shifters. Three types of mixed-voltage I/O buffers have been reported in prior works.

Type I mixed-voltage I/O buffer is able to receive the signals at  $2 \times V_{DD}$ , as shown in Fig. 1 [6]–[9]. By using the stacked NMOS, the gate-oxide overstress at the output NMOS transistor can be avoided when  $2 \times V_{DD}$  is received. Besides, the gate-tracking and floating N-well methodologies are used to remove the unwanted leakage current path through the output PMOS and its parasitic diode, respectively. The mentioned stacked NMOS and leakage elimination methodologies are only activated when  $2 \times V_{DD}$  appears in the receiving mode. Thus, Type I mixed-voltage I/O buffer can only receive the high voltage signal, but it can not transmit a high voltage signal. Let alone a  $2 \times V_{DD}$  signal.

Type II mixed-voltage I/O buffer, which can transmit high voltage signals, was disclosed in Fig. 2[10]–[12]. To avoid the gate-oxide overstress, two individual stacked PMOS and NMOS are used in the output stage. Besides, a level shifter and a bias circuit are employed to provide the appropriate gate bias voltages for the transistors in the output stage. However, these designs overlooked the problem of unwanted leakage current paths when a high voltage signal is biased at the PAD in the receiving mode.

Type III mixed-voltage I/O buffer can transmit and receive signals with high, typical, and low voltage levels ( $V_{DDH}$ ,  $V_{DD}$ , and  $V_{DDL}$ ) by including the mentioned methodologies,

Manuscript received December 28, 2011; revised April 08, 2012; accepted May 05, 2012. This work was supported in part by Metal Industries Research Development Centre (MIRDC) and Ministry of Economic Affairs, Taiwan, under Grant 101-EC-17-A-01-01-1010, 99-EC-17-A-01-S1-104, and 99-EC-17-A-19-S1-133. It was also partially supported by National Science Council, Taiwan, under grant NSC99-2221-E-110-082-MY3, NSC99-2923-E-110-002-MY2, NSC-99-2221-E-110-081-MY3, NSC-99-2220-E-110-001. This research was also partially supported by the Southern Taiwan Science Park Administration (STSPA), Taiwan, under Contract EI-28-05-10-101. This paper was recommended by Associate Editor Massimo Alioto.

C.-C. Wang, C.-L. Chen, H.-Y. Tseng, and H.-H. Hou are with the Department of Electrical Engineering, National Sun Yat-Sen University, 80424, Taiwan (e-mail: ccwang@ee.nsysu.edu.tw).

C.-Y. Juan is with the Metal Industries Research and Development Centre (MIRDC), Taipei 106, Taiwan (e-mail: chunying@mail.mirde.org.tw).

Color versions of one or more of the figures in this paper are available online at <http://ieeexplore.ieee.org>.

Digital Object Identifier 10.1109/TCSI.2012.2215744

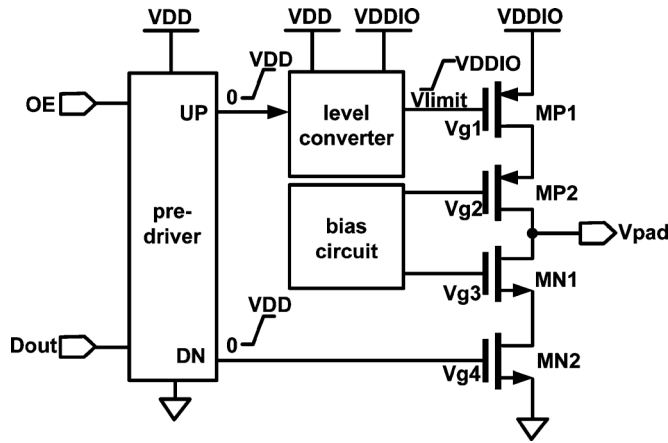


Fig. 2. Type II mixed-voltage I/O buffer with the level converter and bias circuit.

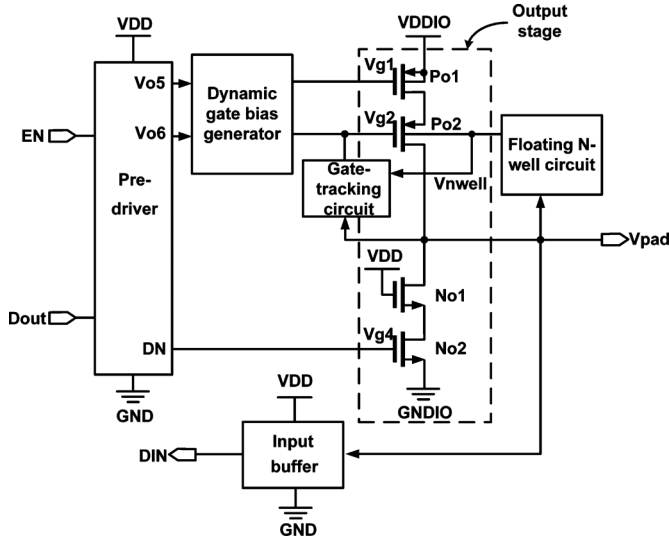


Fig. 3. Type III mixed-voltage I/O buffer with the gate-tracking circuit, floating N-well circuit and dynamic gate bias generator.

as shown in Fig. 3 [1], [13]. However, these reported I/O buffers can only communicate with the signal  $\approx 1/2 \times VDD$ . When the supply voltage (VDDIO) is scaled down to be lower than  $1/2 \times VDD$ , the output signal is difficult to be pulled up to the required I/O voltage (VDDIO) due to the body effect of the output PMOS and the low turn-on voltages ( $V_{gs}$ ) of the output NMOS. On the other hand, the input stages of this type of I/O buffers could not receive the signals with amplitude lower than  $1/2 \times VDD$ . It is the reason why a lower bound of  $1/2 \times VDD$  appears in the state-of-the-art of the mixed-voltage I/O buffers.

Notably, in past several years, many mixed-voltage I/O buffers were reported to deal with the chip interface problems of different voltage levels [14]–[17]. However, the transmitting and receiving frequency of most previously mentioned works are not fast enough to meet the specification of PCI-express, which is up to 266 MHz. Therefore, a wide range I/O buffer with high speed able to simultaneously transmit and receive signal from VDD to  $2 \times VDD$  is very much needed as a total solution for these scenarios.

This work proposes a high speed I/O buffer using 90 nm 1.2 V CMOS process, which can transmit and receive the signal of  $2 \times VDD/VDD$  without any gate-oxide overstress and leakage current. To communicate the signal with  $2 \times VDD$  swing, double stacked transistors and the dual-path gate-tracking circuit are used in the output stage to avoid the gate-oxide overstress. Notably, a simplified floating N-well circuit with low power consumption is adopted to avoid leakage current path produced by parasitic diodes. Meanwhile, no thick oxide layer is used. The higher bound of the operating voltage is expanded to be over  $2 \times VDD$ . The output frequencies for  $VDDIO = 2 \times VDD/VDD$  are measured to be 800/704 Mbps, respectively, at a given capacitive load of 20 pF. Besides, the current drive capability with ESD protection is also justified in this paper.

In Section II, the functions of each block in the bidirectional mixed-voltage I/O buffer are described in detail. In Section III, the proposed dual-path gate-tracking circuit is disclosed, including five modes. In Section IV, the measurement results, including die photo and eye diagrams, are given to justify the function of the proposed design. A brief conclusion is given in Section V.

## II. VDD TO $2 \times VDD$ BIDIRECTIONAL MIXED-VOLTAGE I/O BUFFER

Fig. 4 shows the block diagram of the proposed VDD to  $2 \times VDD$  Bidirectional Mixed-Voltage I/O buffer composed of a Pre-driver, an Input stage, an Output stage, a VDDIO detector, a Vg1 generator, a Floating N-well circuit, and a Dual-path gate-tracking circuit.

### A. Pre-Driver

The details of Pre-driver in Fig. 4 are shown in Fig. 5, which is a decoder circuit to pre-drive Vg1 generator, Dual-path gate-tracking circuit (i.e., OE), and Output stage (i.e., Vg4). When the voltage of control signal (OE) is at logic 1, the I/O buffer enters the transmitting mode (Tx mode). The logic state of Vpad must be determined by DOUT. Besides, the current driving capability of the signal DOUT will be boosted by the Pre-driver to drive these transistors with large dimensions (i.e., Po1, Po2, No2). On the other hand, the I/O buffer is at the receiving mode (Rx mode) given that OE is logic 0. The receiving signal Din would be determined by Vpad. The details of Input stage will be disclosed in the following text. For the sake of clarification, the Boolean equations as well as the functionality of each output signals in Pre-driver are tabulated in Table I.

### B. Output Stage

Since the supply voltage of the core circuit is 1.2 V in 90 nm CMOS process, the output stage must be realized with two stacked PMOS and NMOS, as depicted in Fig. 4. Besides, the appropriate gate voltages are needed for Po1, Po2, No1, and No2 to ensure the gate-oxide reliability and correct functions. The detailed gate drives of the Output stage are tabulated in Table II, including Vg1, Vg2, Vg3, Vg4, and Vnwell, which are described as follows.

Po1: Because the voltage difference between the gate and source ( $V_{gs}$ ) must be smaller than 1.2 V, the Vg1 must be larger than ‘VDDIO–1.2 V’ in Tx mode. By contrast, Po1

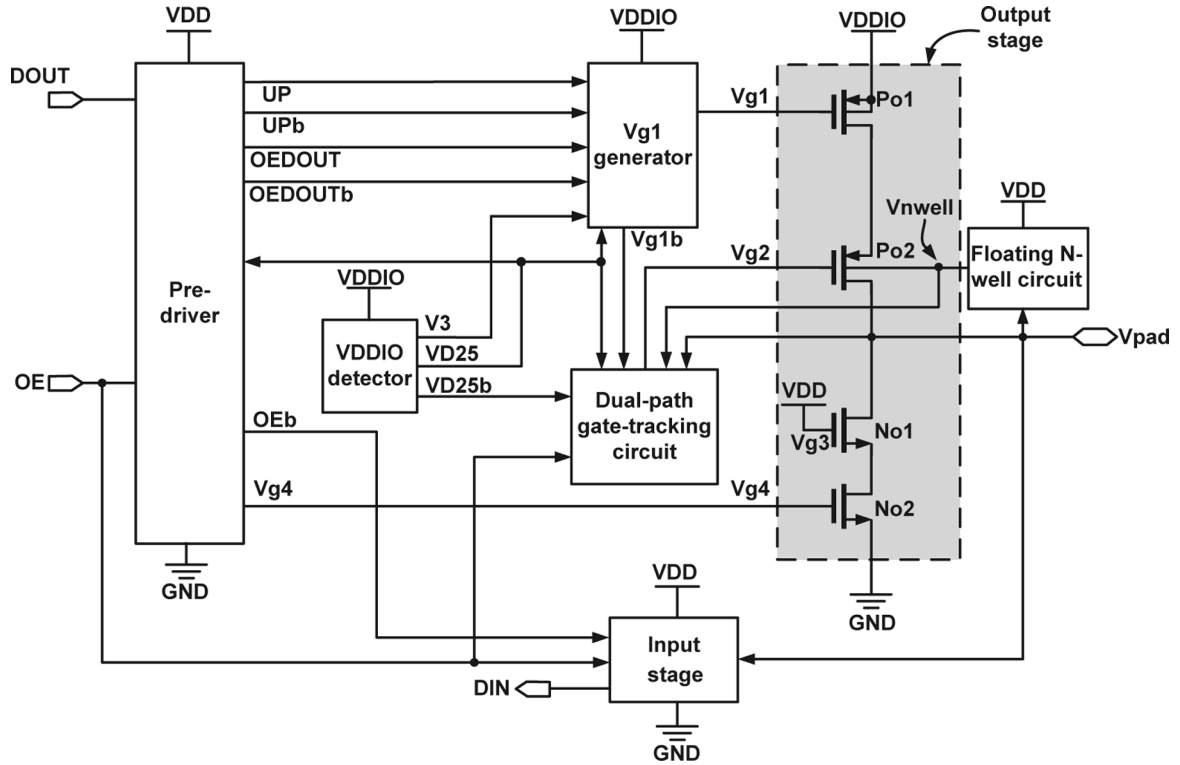


Fig. 4. The proposed mixed-voltage I/O buffer.

 TABLE I  
 FUNCTIONALITY OF EACH OUTPUT SIGNALS OF PRE-DRIVER

Boolean equation	Functionality
OEb	OE
	An inverted OE signal is generated.
OEDOUTb	OE & DOUT
	When I/O buffer is operated in Tx mode, DOUT signal is sent to Vg1 generator.
OEDOUT	OEDOUTb
	An inverted OEDOUTb signal is generated.
Vg4	OE & OEDOUTb
	When I/O buffer is operated in Tx mode, Vg4 signal is the inverted DOUT signal.
UP	VD25 & OEDOUT
	If I/O buffer is operated in $2 \times VDD$ , UP is sent to Vg1 generator.
UPb	UP
	An inverted UP signal is generated.

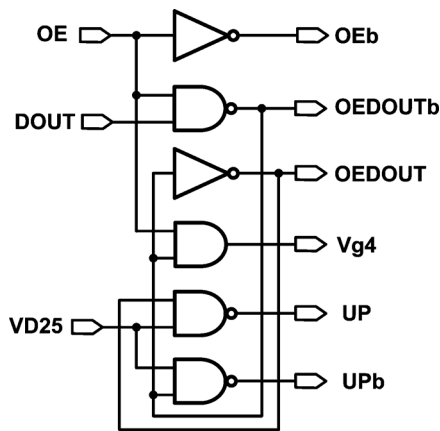


Fig. 5. Pre-driver.

must be turned off in Rx mode, which means the Vg1 must be equal to VDDIO.

Po2: Because the voltage difference between the gate and drain (Vgd) must be smaller than 1.2 V in Tx mode, Vg2 must be in the range between ‘VDDIO—1.2 V’ and

‘1.2 V’. By contrast, the I/O buffer detects the signal with high voltage in Rx mode, Vg2 is set to the same as the voltage of Vpad. Since the voltage difference between the bulk and drain (Vbd) must be smaller than 1.2 V, Vnwell should be varied with Vpad. If Vpad equals to VDDIO, Vnwell is pulled high to VDDIO in Tx mode. On the other hand, if Vpad is 0 V, Vnwell must be pulled low to 1.2 V in Tx mode. In Rx mode, Vnwell behaves like Vg2.

No1: No1 is always turned on in Tx and Rx modes to provide a voltage stress relaxation mechanism from Vpad. Therefore, Vg3 is driven by VDD, which still is in the tolerance of reliability.

No2: Because the Vgd and Vgs must be smaller than 1.2 V in Tx mode, Vg4 must be in the range between ‘VDDIO—1.2 V’ and ‘1.2 V’. Therefore, Vg4 can be directly driven by VDD = 1.2 V. No2 must be turned off in Rx mode when Vg4 is 0 V.

### C. VDDIO Detector

VDDIO detector is mainly implemented using a string of diode-connected PMOS transistors to generate several voltage biases, V1–V6, as illustrated in Fig. 6. When VDDIO is at  $2 \times$

TABLE II  
GATE VOLTAGES OF THE OUTPUT STAGE

	VDDIO (V)	Vg1 (V)	Vg2 (V)	Vg3 (V)	Vg4 (V)	Vnwell (V)
Rx mode	$2 \times VDD$	VDDIO	$VDD/V_{pad}^a$	VDD	0 V	$VDD/V_{pad}^a$
Rx mode	VDD	VDD	VDD	VDD	0 V	VDD
Tx mode	$2 \times VDD$	$> 'VDDIO - 1.2' / VDDIO$	$> 'VDDIO - 1.2' V$	VDD	0 V/VDD	$VDDIO/VDD$
Tx mode	VDD	0 V/VDD	0 V	VDD	0 V/VDD	VDD

<sup>a</sup> When  $2 \times VDD$  is received.

<sup>b</sup> The left side value is that I/O buffer transmits logic 1; the right side value is that I/O buffer transmits logic 0

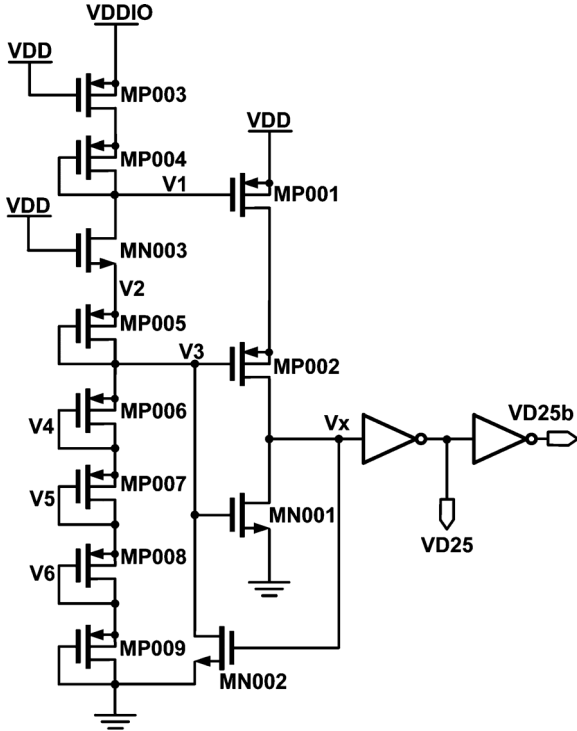


Fig. 6. VDDIO detector.

VDD, MP003 is turned on and V1 is high enough to turn off MP001. To keep the voltage drop between V1 and the voltage of node Vx less than 1.2 V, MP002 is inserted at the drain of MP003. The gate voltage of MP002, V3, is then maintained less than  $'VDD - V_{th_{PM005}}' (\approx 0.8 V)$ , which is the threshold voltage of MP005, to avoid reliability problems. Meanwhile, MN001 is turned on to discharge the voltage of node Vx to 0 V. The state of VD25 is then pulled up to logic 1. On the other hand, when VDDIO is at VDD, MP003 is turned off so that MP001 and MP002 are both turned on to pull up the voltage of node Vx to VDD. The state of VD25 is then pulled down to logic 0. As soon as the voltage of node Vx is up to VDD, MN002 is turned on to shut off MN001 to eliminate the leakage current.

#### D. Vg1 Generator

Referring to Fig. 7, Vg1 generator in Fig. 4 is like a voltage level converter, which generates a pair of complementary signals, Vg1 and Vg1b. Vg1 generator is composed of two cross-coupled PMOS transistors as a latch with stacked NMOS transistors in series as discharging paths. In Rx mode, the

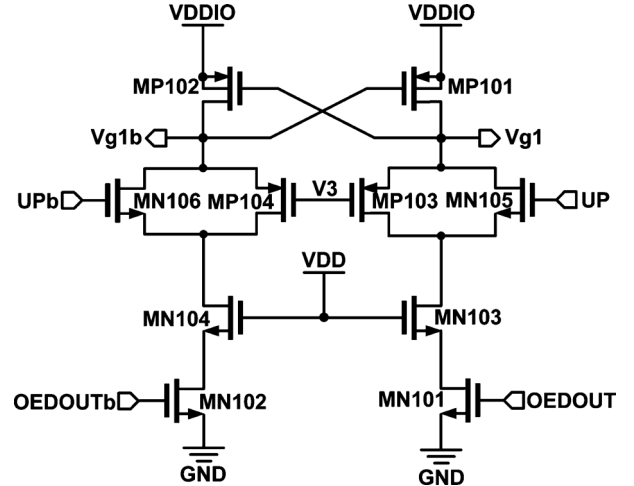


Fig. 7. Vg1 generator.

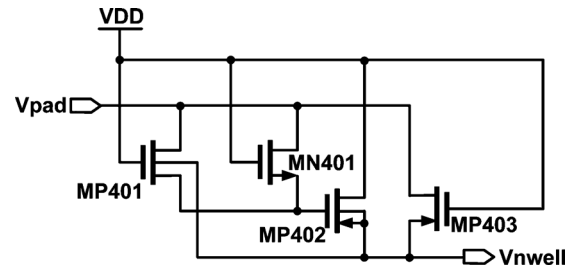


Fig. 8. Floating N-well circuit.

voltage of OEDOUT is biased at 0 V to pull high Vg1 to VDDIO. Thus, Po1 of Output stage in Fig. 4 can be turned off to eliminate the risk of any leakage current. In Tx mode, when VDDIO is  $2 \times VDD$  and the signal Dout is at logic 1, the voltage of OEDOUT is logic 1 to turn on the MN101. Then, Vg1 can be discharged down to  $V3 + V_{th_{PM103}}$  through MP103, MN103, and MN101, where  $V_{th_{PM103}}$  is the threshold voltage of MP103. At the same time, the voltage of OEDOUTb is biased at 0 V, MN102 is turned off to pull Vg1b up to VDDIO, which can also turn off the MP101 to prevent any static leakage current path.

#### E. Floating N-Well Circuit

A simplified floating N-well circuit is adopted in this study, as shown in Fig. 8. When Vpad is higher than VDD, MP403 is turned on. Thus, Vnwell can be charged up to Vpad to avoid



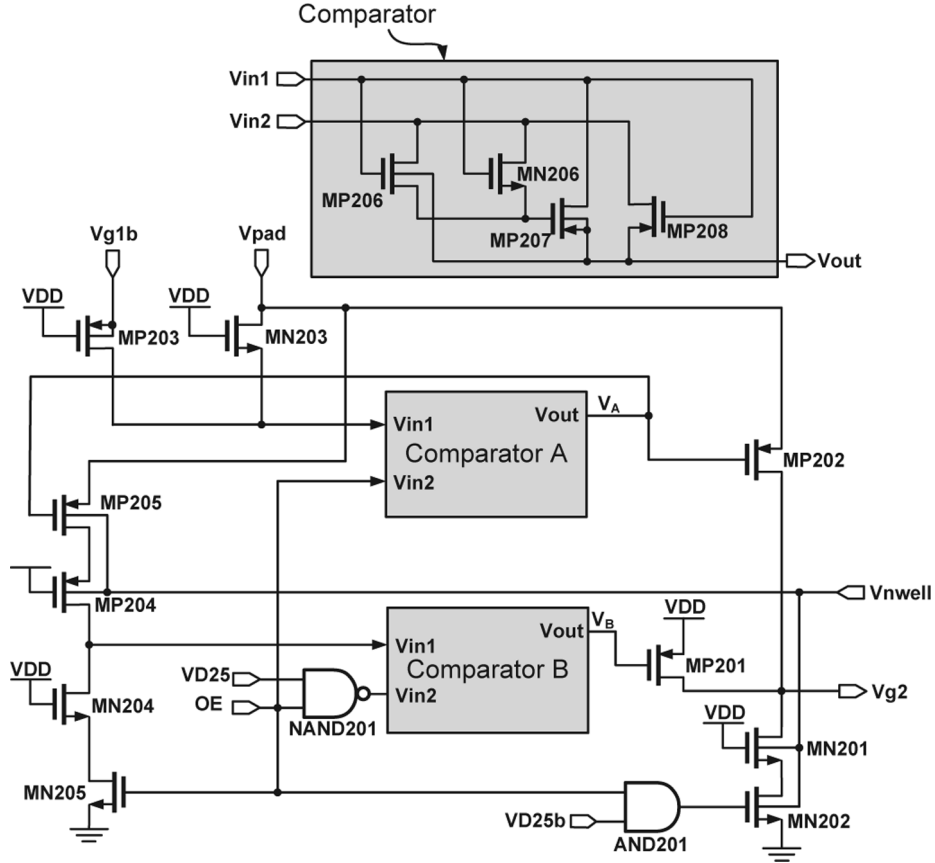


Fig. 11. Dual-path gate-tracking circuit.

is that only one signal path and certain complicated logical circuits based on a large look-up table were used in these prior works for the sake of area cost. Therefore, we propose a dual-path voltage comparison approach in this work to fasten the generation of  $V_{g2}$ .

Referring to Fig. 11, the schematic of Dual-path gate-tracking circuit, namely  $V_{g2}$  generator, in Fig. 4 is revealed, including two Comparators, Comparator A and Comparator B. These comparators are utilized to compare two voltages, which are  $V_{in1}$  and  $V_{in2}$ , and deliver the higher one as  $V_{out}$  (i.e., if  $V_{in1}$  is larger than  $V_{in2}$ ,  $V_{out}$  is equal to  $V_{in1}$ ). Then, there are a total of 5 operation scenarios in Dual-path gate-tracking circuit described as follows.

#### A. Tx Mode and $V_{DDIO} = 2 \times V_{DD}$

When I/O buffer is in Tx mode,  $V_{DDIO}$  is at  $2 \times V_{DD}$ , and  $DOUT$  is at logic 1.  $V_{g1b}$ , biased at  $2 \times V_{DD}$  generated by  $V_{g1}$  generator, is fed into  $V_{in1}$  of Comparator A through MP203. Besides, OE (=VDD) is fed into  $V_{in2}$  of Comparator A. After comparing two voltages by Comparator A, VDD and  $V_{g1b}$  ( $=2 \times V_{DD}$ ), the higher one is presented at node  $V_A$  ( $=2 \times V_{DD}$ ) to turn off MP202. Because the  $V_A$  is  $2 \times V_{DD}$ , MP205 is turned off. Meanwhile, since OE is VDD, MN205 is turned on. Thus, the  $V_{in1}$  of Comparator B is pulled low to 0 V. Because the VD25 is logic 1 generated by VDDIO detector, and OE is logic 1,  $V_{in2}$  of Comparator B is pulled down to 0 V. After comparing two input voltages by Comparator B,  $V_B$  is 0 V to turn on MP201. MN202 is turned off by output

of AND201 because VD25b is logic 0. Therefore,  $V_{g2}$  is pulled high to VDD through MP201.

When  $DOUT$  is at logic 0 and  $V_{pad}$  is 0 V, MP202 is also turned off.  $V_B$  is 0 V to turn on MP201. Thus,  $V_{g2}$  is still kept as VDD through MP201.

#### B. Tx Mode and $V_{DDIO} = V_{DD}$

When I/O buffer is in Tx mode,  $V_{DDIO}$  is at VDD, and  $DOUT$  is at logic 1. Then,  $V_{in1}$  of Comparator A is discharged to VDD. Besides, OE (=VDD) is fed into  $V_{in2}$  of Comparator A. That means  $V_A$  must be VDD to turn off MP202. At the same time, MP205 is turned off. Besides, since OE is VDD, MN205 is turned on. Thus,  $V_{in1}$  of Comparator B is pulled low to 0 V. Simultaneously, since VD25 is logic 0,  $V_{in2}$  of Comparator B is pulled high to VDD. Then,  $V_B$  must be VDD to turn off MP201. MN202 is then turned on by AND201. Therefore,  $V_{g2}$  is pulled low to 0 V through MN201 and MN202.

When  $DOUT$  is at logic 0 and  $V_{pad}$  is 0 V, MP202 is also turned off.  $V_B$  is VDD to turn off MP201. Therefore,  $V_{g2}$  is still 0 V.

#### C. Rx Mode and $V_{pad} = 2 \times V_{DD}$

When I/O buffer is in Rx mode and  $V_{pad}$  is  $2 \times V_{DD}$ ,  $V_{in1}$  of Comparator A is discharged to ' $V_{DD}-V_{th_{MN203}}$ ' through MN203. Besides, OE (=0 V) is fed into  $V_{in2}$  of Comparator A. Therefore,  $V_A$  of Comparator A becomes ' $V_{DD}-V_{th_{MN203}}$ ' to turn on MP202. By AND201, MN202 must be turned off. Therefore,  $V_{g2}$  is pulled high to  $2 \times V_{DD}$  through MP202.

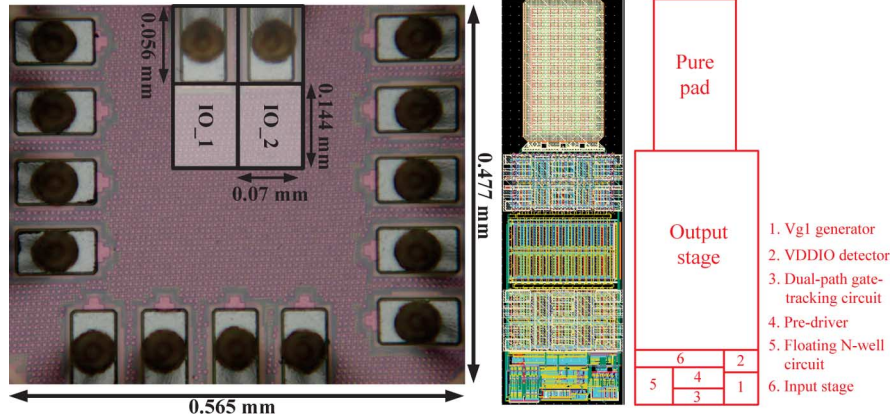


Fig. 12. Die photo of the proposed mixed-voltage I/O buffer.

#### D. Rx Mode and $V_{\text{pad}} = \text{VDD}$

When I/O buffer is in Rx mode and  $V_{\text{pad}}$  is VDD,  $V_{\text{in1}}$  of Comparator A is charged to ' $\text{VDD} - V_{\text{thMN203}}$ ' through MN203. Besides,  $\text{OE} (= 0 \text{ V})$  is fed into  $V_{\text{in2}}$  of Comparator A. Thus,  $V_A$  is ' $\text{VDD} - V_{\text{thMN203}}$ ' to turned on MP202. By AND201, the MN202 must be turned off. Therefore,  $V_{\text{g2}}$  is pulled high to VDD through MP202.

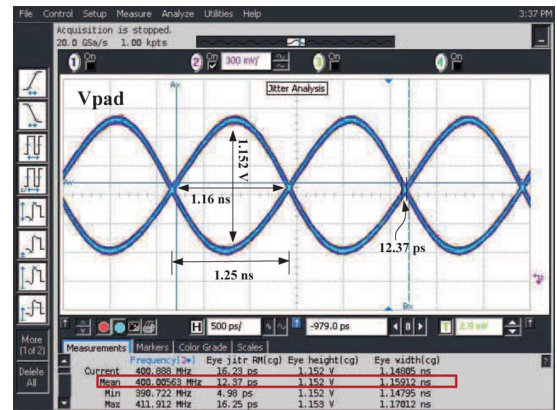
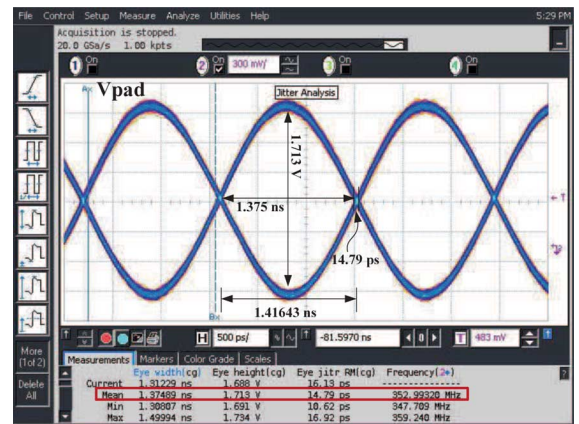
#### E. Rx Mode and $V_{\text{pad}} = 0 \text{ V}$

When  $V_{\text{pad}}$  is 0 V,  $V_{\text{in1}}$  of Comparator A is discharged to 0 V. Then,  $V_A$  must be pulled down to 0 V.  $V_{\text{in1}}$  of Comparator B is discharged to ' $V_{\text{thpMP205}} + V_{\text{dsMP204}}$ ' through MP205 and MP204. Therefore,  $V_B$  is ' $V_{\text{thpMP205}} + V_{\text{dsMP204}}$ ' to turned on MP201. Then,  $V_{\text{g2}}$  is also pulled high to VDD through MP201.

In short, not only the separation of voltage comparison using the dual-path methodology shortens the path to generate appropriate gate drives of MP202, MN202, and MP201, the look-up table required by the prior works [13]–[16] is also drastically reduced.

### IV. IMPLEMENTATION AND MEASUREMENT RESULTS

The proposed design is implemented using a typical 90 nm CMOS process to justify the performance. Fig. 12 shows the die photo of the proposed mixed-voltage I/O buffer. The mixed-voltage I/O buffer's area is  $0.07 \times 0.144 \text{ mm}^2$ , and a mixed-voltage I/O buffer with bounding pad's area is  $0.07 \times 0.2 \text{ mm}^2$ . The eye diagrams of  $V_{\text{pad}}$  given different VDDIO are measured in Tx mode, as shown in Figs. 13 and 14. The performance of the proposed design in Tx mode is summarized in the Table III. The maximum data rate in VDDIO = 1.2 (VDD) and VDDIO = 2.5 V (over  $2 \times \text{VDD}$ ) are 800 Mbps and 704 Mbps, respectively. Fig. 15 depicts the waveform of  $V_{\text{pad}}$  in the Rx mode. The maximum data rate of the proposed design in Rx mode is 660 Mbps. Table IV shows the comparison with several prior works. In terms of voltage modes, our design attains the same  $2 \times \text{VDD}$  functionality as [1], [2], and [14]. Although [15] and [16] reported sub- $3 \times \text{VDD}$  tolerant capability, their data rate are relatively slow. Our design consumes only  $0.09 \mu\text{W}$  and 0.78 mW in static and dynamic power, respectively, to provide 800 Mbps performance. Although this work

Fig. 13. The eye diagram of  $V_{\text{pad}}$  with VDDIO = 1.2 V in Tx mode.Fig. 14. The eye diagram of  $V_{\text{pad}}$  with VDDIO = 2.5 V in Tx mode.

attains the edge of speed at the expense of power consumption, the PDP (power-delay product) outperforms the second fastest work [1] very significantly.

### V. CONCLUSION

A high speed VDD to  $2 \times \text{VDD}$  bidirectional mixed-voltage tolerant I/O buffer is proposed in this paper. The signal with a VDD to  $2 \times \text{VDD}$  swing can be transmitted and received over 660 Mbps data rate. Besides, the effects of gate-oxide overstress and the leakage current are both eliminated. A novel Dual-path

TABLE IV  
PERFORMANCE CAPARISON OF MIXED-VOLTAGE I/O BUFFER WITH PRIOR WORKS

	Year	Voltage modes (V)	Maximum data rate (Mbps)	Process ( $\mu\text{m}$ )	Area ( $\text{mm}^2$ )	Power consumption Static/Dynamic(mW)	Power-delay product (PDP) (pJ)
This work	2011	1.2/2.5	800	0.09	0.01008	0.00009/0.78	0.975
[1]	2008	1.5/3.3	532	0.18	N/A	17.556 (Dynamic)	33
[2]	2009	1.5/3.3	266	0.13	0.0997	N/A	N/A
[14]	2010	0.9/1.2/1.8/2.5/3.3/5.0	158.4	0.35	0.0497	0.00033 (Static)	N/A
[15]	2010	0.9/1.2/1.8/3.3/5.0	100	0.18	0.04082	0.0039 (Static)	N/A
[16]	2011	0.9/1.2/1.8/3.3/5.0	250	0.18	0.044	0.017 (Static)	N/A

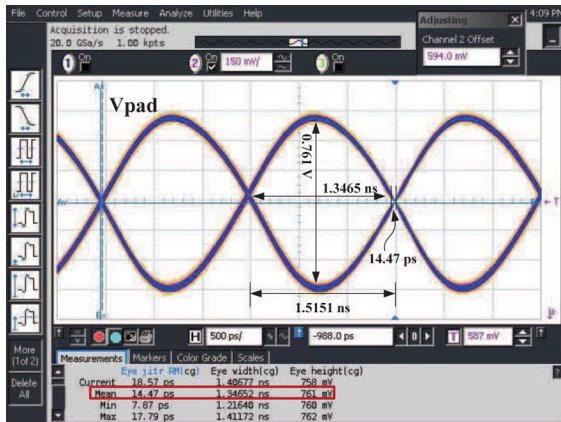


Fig. 15. The eyes diagram of the proposed design in Rx mode.

TABLE III  
PERFORMANCE OF MIXED-VOLTAGE I/O BUFFER WITH DIFFERENT VDDIO IN TX MODE

VDDIO	Maximum data rate	Eye jitter	Eye height	Eye width
1.2 V	800 Mbps	12.37 ps	1.152 V	1.1591 ns
2.5 V	704 Mbps	14.79 ps	1.713 V	1.3749 ns

gate-tracking circuit is proposed to adjust gate drive of Po2 depending in different modes. All of the functions are verified through the on-silicon measurement. The maximum data rate reaches 800 Mbps, which is high enough to meet the specification of PCI-express.

#### ACKNOWLEDGMENT

The authors would like to express their deepest gratefulness to Chip Implementation Center (CIC) of National Applied Research Laboratories (NARL), Taiwan, for their thoughtful chip fabrication service.

#### REFERENCES

- [1] M.-D. Ker, T.-M. Wang, and F.-L. Hu, "Design on mixed-voltage I/O buffers with slew-rate control in low-voltage CMOS process," in *Proc. 15th Int. Conf. Electronics, Circuits and Systems*, Aug. 2008, pp. 1047–1050.
- [2] M.-D. Ker and Y.-L. Lin, "Design of  $2 \times V_{DD}$ -tolerant I/O buffer with  $1 \times V_{DD}$  CMOS devices," in *Proc. IEEE Custom Integrated Circuits Conf. (CICC 2009)*, Sep. 2009, pp. 539–542.
- [3] G. Liu, Y. Wang, and S. Jia, "A new design of mixed-voltage I/O buffers with low-voltage-thin-oxide CMOS process," in *Proc. 7th Int. Conf. ASIC*, Oct. 2007, pp. 201–204.
- [4] M.-D. Ker, S.-L. Chen, and C.-S. Tsai, "Overview and design of mixed-voltage I/O buffers with low-voltage thin-oxide CMOS transistors," *IEEE Trans. Circuits Syst. I: Reg. Papers*, vol. 53, no. 9, pp. 1934–1945, Sep. 2006.

- [5] H.-W. Tsai and M.-D. Ker, "Design of  $2x V_{DD}$ -Tolerant I/O buffer with considerations of gate-oxide reliability and hot-carrier degradation," in *Proc. 14th IEEE Int. Conf. Electronics, Circuits and Systems*, Dec. 2007, pp. 1240–1243.
- [6] C.-H. Chuang and M.-D. Ker, "Design on mixed-voltage-tolerant I/O interface with novel tracking circuits in a  $0.13\text{-}\mu\text{m}$  CMOS technology," in *Proc. IEEE Int. Symp. Circuits and Systems (ISCAS 2004)*, May 2004, vol. 2, pp. 577–580.
- [7] M. J. M. Pelgrom and E. C. Dijkmans, "A  $3/5$  V compatible I/O buffer," *IEEE J. Solid-State Circuits*, vol. 30, no. 7, pp. 823–825, Jul. 1995.
- [8] M.-D. Ker and S.-L. Chen, "Design of mixed-voltage I/O buffer by using NMOS-blocking technique," *IEEE J. Solid-State Circuits*, vol. 41, no. 10, pp. 2324–2333, Oct. 2006.
- [9] M.-D. Ker and F.-L. Hu, "Design on mixed-voltage I/O buffers with consideration of hot-carrier reliability," in *Proc. Int. Symp. VLSI Design, Automation and Test (VLSI-DAT 2007)*, Apr. 2007, pp. 1–4.
- [10] S.-L. Chen and M.-D. Ker, "An output buffer for  $3.3\text{-V}$  applications in a  $0.13\text{-}\mu\text{m}$   $1/2.5\text{-V}$  CMOS process," *IEEE Trans. Circuits Syst. II: Express Briefs*, vol. 54, no. 1, pp. 14–18, Jan. 2007.
- [11] A.-J. Annema, G. J. G. M. Geelen, and P. C. de Jong, " $5.5\text{-V}$  I/O in a  $2.5\text{-V}$   $0.25\text{-}\mu\text{m}$  CMOS technology," *IEEE J. Solid-State Circuits*, vol. 36, no. 3, pp. 528–538, Mar. 2001.
- [12] B. Serneels, T. Piessens, M. Steyaert, and W. Dehaene, "A high-voltage output driver in a  $2.5\text{-V}$   $0.25\text{-}\mu\text{m}$  CMOS technology," *IEEE J. Solid-State Circuits*, vol. 40, no. 3, pp. 576–583, Mar. 2005.
- [13] T.-J. Lee, T.-Y. Chang, and C.-C. Wang, "Wide-range  $5.0/3.3/1.8$  V I/O buffer using  $0.35\text{-}\mu\text{m}$   $3.3\text{-V}$  CMOS technology," *IEEE Trans. Circuits Syst. I: Reg. Papers*, vol. 56, no. 4, pp. 763–772, Apr. 2009.
- [14] C.-C. Huang, T.-J. Lee, W.-C. Chang, and C.-C. Wang, " $(1/3) \times V_{DD}$ -to- $(3/2) \times V_{DD}$  wide-range I/O buffer using  $0.35\text{-}\mu\text{m}$   $3.3\text{-V}$  CMOS technology," *IEEE Trans. Circuit Syst. II: Express Briefs*, vol. 57, no. 2, pp. 126–130, Feb. 2010.
- [15] C.-C. Wang, C.-H. Hsu, and Y.-C. Liu, "A  $1/2 \times V_{DD}$  to  $3 \times V_{DD}$  bidirectional I/O buffer with a dynamic gate bias generator," *IEEE Trans. Circuits Syst. I*, vol. 57, no. 7, pp. 1642–1653, Jul. 2010.
- [16] C.-C. Wang, C.-H. Hsu, S.-C. Liao, and Y.-C. Liu, "A wide voltage range digital I/O design using novel floating n-well circuit," *IEEE Trans. Very Large Scale Integr. (VLSI) Syst.*, vol. 19, no. 8, pp. 1481–1485, Aug. 2011.
- [17] C.-C. Wang, R.-C. Kuo, and J.-W. Liu, " $450$  MHz  $1.0$  V to  $1.8$  V bidirectional mixed-voltage I/O buffer using  $90\text{-nm}$  process," in *Proc. IEEE Int. Conf. IC Design and Technology*, Jun. 2010, pp. 55–58.
- [18] *JEDEC Standard*, JESD8-12A.01, Sep. 2007.



**Chua-Chin Wang** (M'9-SM'04) received the Ph.D. degree in electrical engineering from SUNY (State University of New York) at Stony Brook, NY, in 1992.

He then joined the Department of Electrical Engineering, National Sun Yat-Sen University, Taiwan, and became a full Professor in 1998. He founded the SOC group in the Department of Electrical Engineering, National Sun Yat-Sen University in 2005. He is currently Chairman of this department. His research interests include memory and logic circuit

design, communication circuit design, and interfacing I/O circuits. Particularly, he applies most of his research results on biomedical, memories, consumer electronics, and wireless communication applications, such as implantable ASIC/SOC, DVB-T/H and NTSC TV circuits, low power memory, high speed digital logic, etc.

Prof. Wang has won the Outstanding Youth Engineer Award of Chinese Engineer Association in 1999, and NSC Research Award from 1994 to 1999. In 2000. He co-founded Asuka Semiconductor Inc., which is an IC design house

located in renowned Hsinchu Scientific Park, Taiwan, and became Executive Secretary in 2005. In 2005, he was awarded with Best Inventor Award in National Sun Yat-Sen University, Taiwan. In 2006, he won Distinguished Engineering Professor Award of Chinese Institute of Engineers and Distinguished Engineer Award of Chinese Institute of Electrical Engineering in the same year. He also won Distinguished Electrical Engineering Professor Award of Chinese Institute of Electrical Engineers in 2007. In 2008, he won Outstanding Paper Award of 2008 IEEE Inter. Conf. of Consumer Electronics. In 2009, he again won Best Inventor Award. He was elevated to be Distinguished Professor of National Sun Yat-Sen University in 2010.

Prof. Wang has served as program committee members in many international conferences. He was Chair of IEEE Circuits and Systems Society (CASS) for 2007–2008, Tainan Chapter. He was also the founding Chair of IEEE Solid-State Circuits Society (SSCS), Tainan Chapter for 2007–2008, and the founding Consultant of IEEE NSYSU Student Branch. He is also a member of the IEEE CASS Multimedia Systems & Applications (MSA), VLSI Systems and Applications (VSA), Nanoelectronics and Giga-scale Systems (NG), and Biomedical Circuits and Systems (BioCAS) Technical Committees. He is a senior member of IEEE since 2004. He was Chair of IEEE CASS Nanoelectronics and Giga-scale Systems (NG) Technical Committee for 2008–2009. Since 2010, he has been invited to be Associate Editors of IEEE Trans. on TCAS-I and TCAS-II. Currently, he is also serving as Associate Editor of IEICE Transactions on Electronics, and Journal of Signal Processing. Dr. Wang was General Chair of 2007 VLSI/CAD Symposium. He was General Co-Chair of 2010 IEEE Inter. Symp. on Next-generation Electronics (2010 ISNE). He is General Chair of 2011 IEEE Inter. Conf. on IC Design and Technology (2011 ICICDT), and General Chair of 2012 IEEE Asia-Pacific Conference on Circuits & Systems (2012 APCCAS).



**Chih-Lin Chen** (S'10) was born in Taiwan in 1986. He received the B.S. and M.S. degrees in electrical engineering from National Sun Yat-Sen University, Taiwan, in 2008 and 2010, respectively. He is currently working toward the Ph.D. degree in electrical engineering at National Sun Yat-Sen University.

His current research interests are VLSI design, high-voltage mixed-signal circuit design, and automobile system design.



**Hsin-Yuan Tseng** was born in Taiwan in 1987. He received the B.S. degree in electronic engineering from National Sun Yat-Sen University, Kaohsiung, Taiwan, in 2010, where he is currently pursuing the M.S. degree in electrical engineering. His recent research interest focuses on I/O design.



**Hsiao-Han Hou** was born in Taiwan on November 26, 1986. She received the M.S. degree in electrical engineering from National Sun Yat-Sen University, Taiwan, in 2011.

Since 2011, she has been with Orise Technology Co., Ltd., Hsin-Chu, Taiwan. She is currently working on panel driver design.



**Chun-Ying Juan** was born in Taiwan in 1982. He received the M.S. degree in electrical engineering from National Sun Yat-Sen University, Taiwan in 2008. His recent research interest focuses on high voltage mixed-signal design.